

LBP-CD155 Liposome Nanovaccine Efficiently Resist Colorectal Cancer and Enhance ICB Therapy

Yajuan Yan^{1,*}, Ting Duan^{1,*}, Xiaonan Xue^{1,*}, Xiaojuan Yang², Miao Liu², Bin Ma^{3,4}, Xiangguo Duan², Chunxia Su¹

¹School of Basic Medicine, Ningxia Medical University, Yinchuan, People's Republic of China; ²School of Inspection, Ningxia Medical University, Yinchuan, People's Republic of China; ³Department of Surgery, The First People's Hospital of Yinchuan, Yinchuan, Ningxia, People's Republic of China; ⁴The Second School of Clinical Medicine, Ningxia Medical University, Yinchuan, 750004, People's Republic of China

*These authors contributed equally to this work

Correspondence: Chunxia Su; Xiangguo Duan, Email chunxiasu@qq.com; duanxiangguo@nxmu.edu.cn

Background: Colorectal cancer (CRC) is a highly malignant and aggressive gastrointestinal tumor. Due to its weak immunogenicity and limited immune cell infiltration lead to ineffective clinical outcomes. Therefore, to improve the current prophylaxis and treatment scheme, offering a favorable strategy efficient against CRC is urgently needed.

Methods: Here, we developed a nanovaccine (LBP-CD155L NVs) loaded with CD155 gene in liposome, which was modified by Lycium barbarum polysaccharides (LBP) through electrostatic interaction. The nanovaccine was characterized by transmission electron microscopy and Zetasizer. It was evaluated in vitro, where NVs facilitated the endocytosis and maturation of DCs, and in vivo, where NVs improved the efficacy of prophylaxis and therapy. In addition, further confirmed the mechanisms by how TLR4 and MGL synergistic pathway endow the nanovaccines towards dendritic cells (DCs). Finally, the safety and tumor immunosuppressive microenvironment were evaluated in the CRC tumor-bearing mouse model.

Results: We successfully developed a nanovaccine that facilitates the endocytosis and maturation of DCs via a synergistic pathway involving TLR4 and MGL, which endow the nanovaccines towards dendritic cells (DCs) and promote the differentiation, thereby enhancing the cytotoxicity of CD8⁺T cells. Consequently, LBP-CD155L NVs can potentiate the efficacy of prophylactic and therapeutic administration in a mouse CRC model, as evidenced by decreased infiltration of myeloid-derived suppressor cells (MDSCs) and Tregs, reprogrammed the macrophage phenotypes, which promoted polarization from M2-like macrophages to M1-like macrophages, increased infiltration of effector T cells. Prophylactic and therapeutic combination regimens with anti-PD-1 treatment demonstrate synergism that stimulates T-cell infiltration into tumors and counteracts immunosuppression, leading to remarkable tumor remission and enhancing the efficacy of immune checkpoint therapy in solid tumors.

Conclusion: Our work provided that LBP-CD155L NVs may serve as a promising tool for reversing tumor immunosuppressive microenvironment and enhancing ICB therapy in CRC.

Keywords: *Lycium barbarum* polysaccharides, nanovaccines, nanovaccine codelivery, CD155, tumor immunotherapy

Introduction

Tumor immunotherapy holds potential as a strategy for controlling and eliminating tumors through the reinitiation and maintenance of tumor-immune circulation, thereby restoring the normal anti-tumor immune response.¹ Currently, the most recognized immunotherapy method for cancer in clinical practice targets the PD-1/PD-L1 or CTLA4 immune checkpoints to relieve immune suppression in tumor micro environment (TME) and subsequently to enhance cytotoxic effect of CD8⁺T cells.² Immune checkpoint blockade (ICB) also reduce infiltrated immune suppressor cells in TME, such as myeloid-derived suppressor cells (MDSCs), regulatory T cells (Tregs) and tumor-associated monocytes or neutrophils, which blocking antitumor immunity.³

Colorectal cancer (CRC) has become a key public health issue,⁴ PD-1 blockers, although in the field of tumor treatment show encouraging effect, however, clinically, for mismatch repair-proficient (pMMR) colorectal tumor cells express weak immunogenicity and infiltrate a limited number immune cells, which makes it difficult to induce an adequate immune response.⁵ Therefore, ICB therapy is ineffective in such patients. In order to increase immunotherapy sensitivity, combined treatments are required to enhance tumor immunogenicity.

In recent years, a large number of immunosuppressive targets have been identified on tumor cells.⁶ One attractive target is cell adhesion molecule CD155 (Poliovirus receptor),⁷ which is commonly over-expressed in tumor cells;⁸ CD155 contributes to tumor cellular proliferation, migration, contract inhibition, and survival, thereby associated with tumor progression, invasion, and metastasis.⁹ CD155 can interact with at least three lymphocyte-expressed receptors: DNAX Accessory Molecule-1 (DNAM-1) or CD226, TIGIT and CD96 on T and NK cells.^{10–12} The inhibitory checkpoint receptors TIGIT and CD96 compete with the co-stimulatory receptor DNAM-1 for binding to CD155, thereby modulating the function of tumor-infiltrating lymphocytes,¹³ and then inducing immunosuppressive effect in TME for many solid tumor indications.¹² The significant immune suppression induced by CD155, along with its very broad expression distribution in cancer, highlights its potential as a therapeutic target for designing cancer vaccines.¹⁴

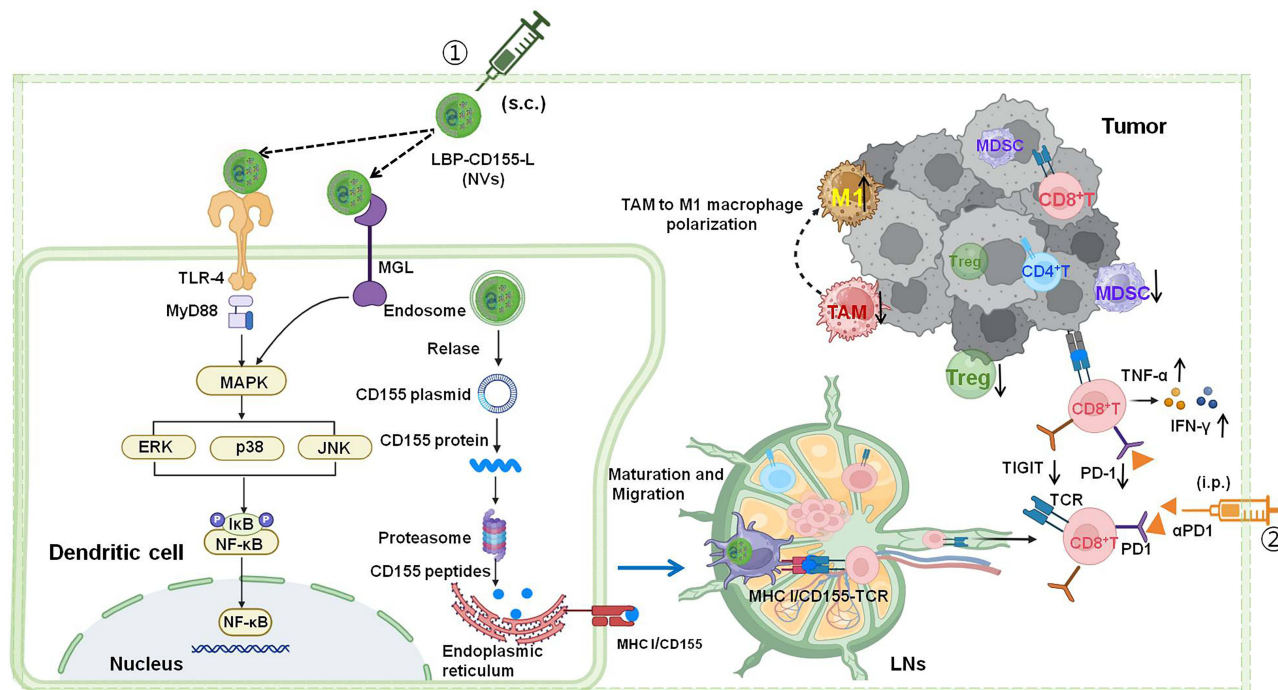
The nanoparticles have been used as vehicles for cancer vaccines to enhance the biocompatibility and efficiency of vaccines, including lipid nanoparticles,¹⁵ polyethylenimine (PEI) nanoparticles,^{16,17} poly (lactic-co-glycolic acid) (PLGA) nanoparticles and so on.^{18,19} To achieve a novel therapeutic approach, we hypothesized that cancer vaccines that deliver CD155 gene to dendritic cells (DCs) and consequent T-cell priming and activation, thereby potentiate the antitumour responses. Here, we designed liposome nanoparticles loaded with CD155 gene.

In many cases, vaccines only stimulate weak immunogenicity to prevent infection.²⁰ Therefore, vaccine adjuvants are required in the preparation of vaccine to boost the immune response.²¹ Polysaccharides belong to a class of natural polymers consisting of glycosidically linked carbohydrate monomers.²² Polysaccharides can activate macrophages, T lymphocytes, B lymphocytes and NK cells, and promote the secretion of immune-related molecules, such as cytokines, antibodies and complement molecules.²² Polysaccharide derivative, monophosphoryl lipid A, has been shown to be a virulent and immunologically active adjuvant by binding to toll-like receptor 4 (TLR4).²³ As vaccine adjuvants, polysaccharides can not only promote antigen-specific immune system but also enhance the body's natural immune function.²⁴ Polysaccharide adjuvants mainly include dextran, chitosan, galactose, mannose and Chinese medicinal herb polysaccharide, such as *Lycium barbarum* polysaccharide (LBP).²⁵ LBP has unique features compared to other polysaccharides and carriers. Dextran has good solubility and biocompatibility but weak targeting specificity, lower targeting efficiency in drug delivery, and a simpler and less intense immune activation pathway than LBP. Chitosan has limited targeting to lesions and activates the immune system differently and less effectively. Galactose-modified liposomes that target liver cells specifically are more efficient in liver-targeted delivery but less in others, and lack direct immune activation. Mannose-modified nanoparticles target specific immune cells effectively. LBP is the major biological active ingredient of the Chinese wolfberry,²⁶ comprises at least six types of monosaccharides such as arabinose, glucose, galactose, mannose, xylose, and rhamnose, and manifests a variety of biological and pharmacological functions, such as antioxidant, anticancer and antiradiation activities,^{27,28} also demonstrating significant immune enhancement effect via regulating the functions of T cells, NK cells, macrophages, and DCs.^{29,30} LBP has a more complex mechanism and acts more comprehensively on the immune system. These unique traits of LBP support its applications. To improve immunotherapy strategies, this article intends to study a tumor vaccine nanoparticle LBP-CD155L NVs with LBP as an adjuvant, that is, a liposome nanoparticle loaded with CD155 gene and modified by LBP to enhance the immune response.

Enhancing the ability of nanoparticles to target antigen presenting cells (APCs) represents a method to improve antigen internalization and thus promote immune response.³¹ APCs express multiple types of lectins on their surface, such as dendritic cell-specific intercellular adhesion molecule-3- grabbing nonintergrin (DC-SIGN), mannose receptors (MR), and galactose type lectins (MGL).^{32,33} These lectins can specifically recognize corresponding glycosyl-modified antigen carriers, improving antigen internalization efficiency.³⁴ Our previous studies indicated that LBP, as a novel

polysaccharide immune adjuvant, could promote maturation of DCs through the TLR4 signal pathway and then activate T cells. Based on its composition, it is speculated that LBP could specifically bind to saccharide receptor on APC surface, mediating the internalization of the liposome nanoparticles loaded with the CD155 gene to enhance APC-targeting. Then, we designed a new liposomal nano vaccine, LBP-CD155L NVs, to provide a new idea for immunotherapy of colorectal cancer. If the LBP-coated liposomal antigen peptide can achieve the desired effect, it can activate the immune system. In vitro, NVs can promote the maturation of lymphocytes and DCs. They enable high expression of MHC class I and II molecules, costimulatory molecules CD80 and CD86 on the DC surface. Moreover, they enhance the secretion of cytokines IL-6 and IL-12p40 by DCs. Mature DCs can then induce the activation of CD8⁺ T cells and upregulate the secretion levels of cytokines such as IFN- γ and TNF- α . In vivo, multiple parameters are considered. The status of CD4⁺T and CD8⁺T, PD-1 and TIGIT expression of CD8⁺T and its secreted TNF- α and IFN- γ and on the surface of CD8⁺T. Meanwhile, the changes in the number of immune suppressive cells in the immune microenvironment such as Tregs, MDSCs, as well as tumor-associated M1 type macrophages can also influence the antitumor immune response. Moreover, the expression levels of cell proliferation marker Ki67 and the apoptosis marker Caspase 3 in mouse tumor tissue could also suggest a potential role of combination therapy in the antitumor effect, which together provide a comprehensive evaluation of the treatment effect.

Overall, this strategy presents (Scheme 1) the following advantages: (1) The nanovaccines are composed of DNA and LBP, which are bio-safe and biodegradable; (2) LBP endows nanovaccines with targeting and stimulating maturation towards APC; (3) NVs loaded with CD155 gene could mediate CD8⁺T cells effect and reverse immunosuppression; (4) The combined NVs and α PD-1 strategy may alleviate and inhibit tumor growth by inducing anti-tumor immune response and inhibiting immune suppressor in TME, which provides a potentially effective approach for clinical tumor immunotherapy.



Scheme.1 Schematic illustration of immunization Lycium barbarum polysaccharide modified nanovaccine and α PD-1 for modulating immune response and immunosuppression to boost cancer immunotherapy.

Materials and Methods

Materials

Soya Lecithin was acquired from Solarbio Co., Ltd. (Beijing, China). Cholesterol was procured from Sigma (USA). Lycium barbarum polysaccharides (LBP) with 98% purity were obtained from Ciyuan Biological Products Co., Ltd. (Shaanxi, China, No. CY190218). Competent *Escherichia coli* DH5 α cells were sourced from TRAN. HT-29 cells were purchased from American type culture collection (ATCC), (Manassas, VA). Recombinant murine granulocyte-macrophage colony-stimulating factor (GM-CSF, 315–03) and recombinant murine interleukin-4 (IL-4, 214–14) were purchased from PeproTech. A comprehensive array of fluorescence-activated cell sorting (FACS) antibodies was procured from BioLegend, including FITC anti-mouse CD8, FITC anti-mouse CD4, FITC anti-mouse CD11c, PerCP-Cy5.5 anti-mouse CD80, BV421 anti-mouse CD86, PE anti-mouse MHC I, V500 anti-mouse MHC II, Alexa Fluor™ 700 anti-mouse CD11b, APC anti-mouse XCR-1, BV510 anti-mouse CD25, PerCP-Cy5.5 anti-mouse FOXP3, PE anti-mouse CD206, APC anti-mouse GR-1, eFluor™ 450 anti-mouse TNF- α , PerCP-Cy5.5 anti-mouse IFN- γ , APC anti-mouse PD-1, PE anti-mouse Tigit, Alexa Fluor™ 700 anti-mouse CD44, and APC-eFluor™ 780 anti-mouse CD62L. The utilization of these antibodies was in strict accordance with the manufacturer's instructions. Additionally, uncoated ELISA kits for mouse tumor necrosis factor-alpha (TNF- α), interferon-gamma (IFN- γ), interleukin-12 (IL-12), and interleukin-6 (IL-6) were acquired from BioLegend and employed following the specified protocols provided by the manufacturer.

Preparation of Cationized LBP

The cationized LBP was prepared by the reductive amination method. First, LBP (0.017 g, equivalent to 3.125 mmol of glucose units) was solubilized in 50 mL of deionised distilled water (DDW). Then, potassium periodate (0.716 g, io4-/sugar molar ratio of 1:1) was added. The mixture was quickly placed in a dark environment and stirring for 72h at room temperature. The resulting polyaldehyde derivative was dialysed with DDW for 48h. After freeze-drying, oxidised LBP was obtained. Oxidized LBP (0.3 g) was dissolved in 20 mL of freshly prepared hydroxylamine hydrochloride water solution (0.25 M, pH 4). This solution was gently stirred overnight at room temperature and then titrated with a standardised sodium hydroxide solution (0.1 M) until an end point was reached as determined by a digital pH meter. Subsequently, 50 mL of oxidised LBP solution was slowly added to an alkaline solution containing a 1.25 equimolar amount of spermine (8.46 mmol), and then dissolved in 30 mL of borate buffer (0.1 M, pH 11) and stirred at room temperature for 24h. Finally, Sodium borohydride (NaBH₄) (0.6 g) was added to the mixture and react for 48h. The resultant light-yellow solution was subjected to dialysis against DDW for 48h. Following freeze-drying, cationized LBP was obtained, completing the synthesis process.

Preparation and Characterization of LBP-CD155L NVs

Cholesterol (30 mg) and soybean lecithin (60 mg), were mixed in a 1:2 mass ratio in 50mL round bottom flask and subsequently dissolved in 10mL chloroform, setting it at moderate speed for a 2.5-hour cycle on a magnetic stirrer at ambient temperature. Then, round bottom flask was moved to the rotary evaporator, 40°C, the chloroform was evaporated by rotation under vacuum, until the mixture is in a “gelatinized” state, 6mL pcDNA3.1⁺-CD155(forward primer 5'-cgGCTAGCATGGCCCGAGCCATGG-3' and reverse primer 5'-ccAAGCTTTCACCTTGTCCTCTGTCTG-3') within PBS was added, continue to be evaporated by rotation for 1h, forming liposome (L) loaded with CD155 gene (CD155-L). The entrapment rate of the pcDNA3.1⁺-CD155 was determine by DNA detecto (SNano-800 Ultra-micro Spectrophotometer). CD155 Mixing CD155L and equal volume of cationized LBP, which was stirred at room temperature for 30 minutes, CD155-L was modified by LBP through electrostatic interaction, forming nanovaccine (LBP-CD155-L NVs). The presence of LBP was quantified using the phenol-concentrated sulphuric acid method, and the binding rate (BR) of LBP to nanoparticles was evaluated. NVs were filtered through a filter of 0.22 μ M, then was freeze-dried for storage.

The nanoparticles, including L, LBP-L, CD155-L, and LBP-CD155-L were individually diluted in deionized water. The particle size, zeta potential, and polydispersity index (PDI) of nanoparticles were analyzed by Zetasizer (Zetasizer

Nano S, Malvern, UK). The morphology and structural attributes of nanoparticles were observed by Transmission Electron Microscopy (TEM, H-7650, Hitachi, Japan).

In Vitro Cytotoxicity of LBP-CD155L NVs

The cytotoxicity of LBP-CD155-L NVs was assessed through CCK-8 assays. Briefly, BMDC were initially seeded into 96-well plates (8×10^5 cells/well) for 24h in 1640 medium. Then incubated with various concentrations of LBP-CD155L (concentration: 200, 150, 100, 50, 25 $\mu\text{g}/\text{mL}$). Inverted microscopy (Olympus, Japan) was used to observe general morphological changes of the BMDC cells, and then the CCK-8 assay was performed and the optical density (OD) values were measured at 450 nm. The cell viability was calculated as follows: $(\text{OD of experimental group} - \text{OD of blank group}) / (\text{OD of negative control group} - \text{OD of blank group})$.

DCs Targeting, Activation Assays and Immunization Studies

Uptake of LBP-L in DCs

To assess the targeting efficacy of LBP-L on DC2.4 cells, the cationized LBP conjugated with fluorescein isothiocyanate (FITC), while the cell membranes were marked with DiI. DC2.4 cells plated in six-well plates were added with LBP-L after fluorescent dye was labeled and incubated at 37°C for 12h. After three washes with phosphate-buffered saline (PBS), the cells were fixed with 4% paraformaldehyde for 30 min, and the cell nuclei were stained with 4', 6-diamidino-2-phenylindole (DAPI; Sigma-Aldrich). Finally, the cells were imaged by fluorescence microscopy (Eclipse 80i; Nikon, Tokyo, Japan).

Maturation of BMDCs

To determine whether LBP-CD155-L nanovaccines treatment could activate DC mature in vitro, both flow cytometry and ELISA kits were employed in this experiment. Immature BMDCs were prepared by the standard protocol and cultured in RPMI 1640 complete medium supplemented with granulocyte-macrophage colony-stimulating factor (GM-CSF; 20 ng/mL) and interleukin-4 (IL-4; 20 ng/mL). The medium was refreshed on days 2 and 4 of the culture. On day 6, cells were harvested and resuspended in RPMI 1640 medium at a density of (5×10^5 cells/well). Subsequently, the cells were incubated with 200 $\mu\text{g}/\text{mL}$ concentrations of L, LBPL-L and LBP-CD155-L for 24h at 37°C , untreated liposome nanoparticles L served as a blank control.

Afterward, the cells were stained with a combination of fluorescently labelled antibodies targeting CD11c, CD80, CD86, MHC-I and MHC-II and analysed by CytoFLEX S flow cytometry. The levels of Interleukin-6 (IL-6) and Interleukin-12p40 (IL-12p40) were measured by ELISA kits according to the instructions provided by the manufacturer. All samples were measured in triplicate.

Nanovaccine Activate Naive CD8^+ T Cells

Immature BMDCs were co-cultured with L, LBPL-L CD155-L and CD155-LBP-L for 48h. Subsequently, nanoparticle-pulsed BMDCs were then co-cultured with mouse spleen lymphocytes at a ratio of 1:10 for an additional 48 h. The expression levels of CD8^+ T cells, $\text{IFN-}\gamma^+\text{CD8}$ T cells, and $\text{TNF-}\alpha^+\text{CD8T}$ cells were detected by flow cytometry. Untreated liposome nanoparticles L served as a blank control.

The Killing Effect of Activated CD8^+ T Cells on HT-29 Cells

We co-incubated the above activated lymphocytes with HT-29 cells at 20:1 for 48h, and used CCK8 to detect the killing effect of activated lymphoid fine on HT-29 cells.

Western Blot Analysis

Proteins were extracted using the radioimmunoprecipitation assay (KGI Biologicals, Inc, Jiangsu, China). The total protein concentrations were measured using the bicinchoninic acid (BCA) protein assay kit (KGI Biologicals, Inc, Jiangsu, China). In brief, 25 μg of proteins were loaded into each lane of sodium dodecyl sulfate polyacrylamide gels, separated by 8% sodium dodecyl sulfate-polyacrylamide gel electrophoresis (SDS-PAGE) gels and transferred onto the polyvinylidene difluoride (PVDF) membrane (Millipore, USA). After blocking with 5% fat-free milk for 2 h, the PVDF

membranes were incubated with the following primary antibodies: Anti-MGL antibody (1:1,000) (cat. no. GR3397231-1; Abcam, UK), anti-TLR4 antibody (1:1,000) (cat. no. sc-293072GR3397231-1; Santa Cruz, USA), anti-Erk1/2 antibody (1:1,000) (cat. no. ab4695S; Cell Signaling Technology, USA), anti-phospho-Erk1/2 antibody (1:1,000) (cat. no. 4376S; Cell Signaling Technology, USA), anti-P38 antibody (1:1,000) (cat. no. 8690S; Cell Signaling Technology, USA), anti-phospho-P38 antibody (1:1,000) (cat. no. 4092S; Cell Signaling Technology, USA), anti-JNK antibody (1:1,000) (cat. no. 9252S; Cell Signaling Technology, USA), anti-phospho-JNK antibody (1:1,000) (cat. no. 4668S; Cell Signaling Technology, USA), anti-NF- κ B antibody (1:1,000) (cat. no. 8242S; Cell Signaling Technology, USA), and anti-phospho NF- κ B antibody (1:1,000) (cat. no. 3033S; Cell Signaling Technology, USA). After three washes with tris-buffered saline containing Tween[®] 20 (TBST), the PVDF membranes were incubated with secondary antibodies GAPDH peroxidase-linked Ab (ZSGB-BIO Technology Co., Ltd., Beijing, China; 1:5000) at room temperature (about 25°C) for 1 h. The gray value of protein bands, utilized to assess protein expression levels, was analyzed using Image-Pro Plus software.

RNA Extraction and RT-qPCR

Total RNA was extracted from samples using the RNAsimple Total RNA Kit (TIANGEN, Shanghai, China), and then transcribed into complementary DNA (cDNA) using a RevertAid First Strand cDNA Synthesis Kit (ThermoFisher Scientific, USA). Reverse transcription quantitative polymerase chain reaction (RT-qPCR) was conducted on an ABI7500 system using a SuperReal PreMix Plus (SYBR Green) (TIANGEN, Shanghai, China) in accordance with the manufacturer's instructions.

In Vivo Immunization and Cancer Immunotherapy Studies

All the mice used for immunological investigations were 6–8-week-old C57BL/6 males. Animals care and treatment procedures were conducted in strict adherence to the guidelines and approvals set by the Institutional Animal Care and Use Committee of Ningxia Medical University. Tumor volume throughout this study was determined by the formula: tumor volume = length \times width² \times 0.5. Animals were euthanized when the tumour masses reached 1.5 cm in diameter or when the animals became moribund with severe weight loss or ulceration. The C57BL/6 mice were automatically divided into seven groups with eight heads for each group. These groups received various immunization formulations. On day 35, after the mice were euthanized, the tumors, spleens and inguinal lymph nodes were extracted and analyzed by a Flow Cytometer.

Firstly, the preventive and therapeutic effects of nanovaccines alone on HT-29 colorectal cancer were evaluated. For the NVs prophylactic group, the mice were immunized with 200 μ g LBP-CD155-L NVs thrice with once a week interval, 7 days after the final immunization, 100 μ L of 3D gelatin microcarriers³⁵ loaded HT-29 cells (1×10^6 cells) were subcutaneously inoculated into the dorsal region of the mice, and tumour growth was monitored every other day. Conversely, in the NVs therapeutic group, a subcutaneous colorectal cancer model utilizing HT-29 cells was established prior to intervention. Mice treated with PBS served as a negative control. Commencing on day 7 post-tumor establishment, the mice received three weekly immunizations with LBP-CD155-L NVs. Tumor size and body weight were systematically recorded starting from day 7. On day 35, after the mice were euthanized, the tumors, spleens and inguinal lymph nodes were extracted and analyzed by a Flow Cytometer.

Subsequently, an investigation was carried out to assess the combined preventive and therapeutic efficacy of LBP-CD155-L NVs and antibodies targeting PD-1 (a PD-1), a known immunosuppressor, against colorectal cancer. The mice were allocated into four groups, each comprising eight subjects. For the control group, PBS was administered throughout the duration of the study. In the aPD-1 group, the PD-1 antibody treatment was delivered intraperitoneally on the 7th, 14th, 28th, 31st, and 34th days following the inoculation of tumor cells into the mice. In the NVs therapeutic+aPD1 group, LBP-L-CD155-L NVs were administered subcutaneously to the mice on the 7th, 14th, and 28th days following tumor implantation, whereas aPD1 was injected intraperitoneally on the 7th, 14th, 28th, 31st, and 34th days as part of the therapeutic regimen. In the NVs, prophylactic+NVs therapeutic+aPD1 treatment group, immunization was carried out similarly with 200 μ g LBP-CD155-L NVs. After the final immunization and a lapse of 7 days, 100 μ L 3D gelatin microcarriers³⁵ loaded HT-29 cells (1×10^6 cells) were introduced into the right scapular region. Following this, The

PD-1 antibody treatment was delivered intraperitoneally on days 7, 14, 28, 31, and 34 after tumor cell inoculation, while LBP-CD155-L NVs were administered subcutaneously on the 7th, 14th, and 28th days following the inoculation.

In Vivo Phenotypic and Functional Assessment of Immune Cells

After the mice were euthanized, the tumors, spleens, and inguinal lymph nodes from the mice were harvested and processed into single-cell suspensions. Subsequently, these cells were passed through 300-mesh screens and subjected to washing with cold phosphate-buffered saline (PBS). After centrifugation, cells were resuspended in 100 μ L of cold PBS and treated with 10 μ L of fluorescently labeled antibodies for an incubation period of 30 minutes at 4°C. Finally, the cells were washed twice and the percentages of various immunocytes were assessed via flow cytometry.

Safety Evaluation

Tumor-bearing mice were treated and sacrificed at the designated time points. The main organs heart, liver, spleen, lung, and kidney were extracted and immersed in paraformaldehyde for 48 h. The fixed tissues were thereafter embedded in paraffin, and histological sections of 5 μ m thickness were prepared. These sections were stained with hematoxylin and eosin (H&E) and then subjected to microscopic examination and photography.

Statistical Analysis

Calculations were performed using GraphPad Prism version 5.0. Statistical analysis was performed using a Student's *t*-test, and the differences between test and control groups were judged to be significant at $0.01 < *P < 0.05$ and extremely significant at $**P < 0.01$, $***P < 0.001$ and $****P < 0.0001$.

Results and Discussion

Preparation and Characterization of LBP Modified NVs

The liposome nanoparticles loaded with CD155, which modified by LBP (LBP-CD155-L NVs) were successfully synthesized (Figure 1A). Nanoparticles presented average hydrodynamic diameters ranging from 122.26 ± 8.15 nm to 165.96 ± 18.34 nm (Figure 1B). Homogeneous spherical particles with a visible lipid layer of nanoparticles were observed under TEM (Figure 1C). The electrification performance of nanoparticles was evaluated by zeta potential assay, which showed transformation into positively charged nanoparticles for LBP-L and LBP-CD155-L, indicating the successful binding of LBP on liposome nanoparticles (Figure 1D). The safety of LBP-CD155-L was evaluated using a CCK-8 assay in mouse bone marrow-derived dendritic cells (BMDCs), demonstrating that LBP-CD155-L did not affect DC viability in the concentration range tested (Figure 1E), and LBP-L was successfully uptaken by DC was observed under immunofluorescence microscopy (Figure 1F), thereby supporting their physiological biocompatibility. The entrapment efficiency (EE%) of CD155 and the binding rates of LBP are shown in [Supplementary Table 1](#). Stability of nanovirines was tested after saving for different days ([Supplementary Table 2](#)).

Intracellular Uptake and DCs Maturation Induced by LBP Modified NVs

Maturation of DCs are essential prerequisites for initiating and directing adaptive immune response.³⁶ The cells surface markers indicating mature BMDCs were detected by flow cytometry following a 24-hour incubation with nanoparticles. The mature BMDCs were identified by gating for CD11c⁺ and CD86⁺, CD80⁺, MHC1⁺, MHCII⁺, respectively. It was shown that nanoparticles modified with LBP significantly increase the expression of activation/maturation markers on the DC surface compared with liposomes without LBP modification (Figure 2A). This finding suggests the superior ability of LBP-modified nanoparticles in targeting and promoting DC maturation. Furthermore, the levels of IL-6 and IL-12p40 in the supernatants were quantified via ELISA, demonstrating that LBP-modified nanoparticles also increased the secretion of these cytokines (Figure 2B), which are implicated in T-cell recruitment and differentiation, as well as in the suppression of regulatory T (Treg) cells.^{37,38}

Our previous studies found that LBP as a novel adjuvant could promote maturation of DCs through the TLR4-MAPK signaling pathway. Containing different monosaccharides such as galactose and mannose, it was speculated that LBP

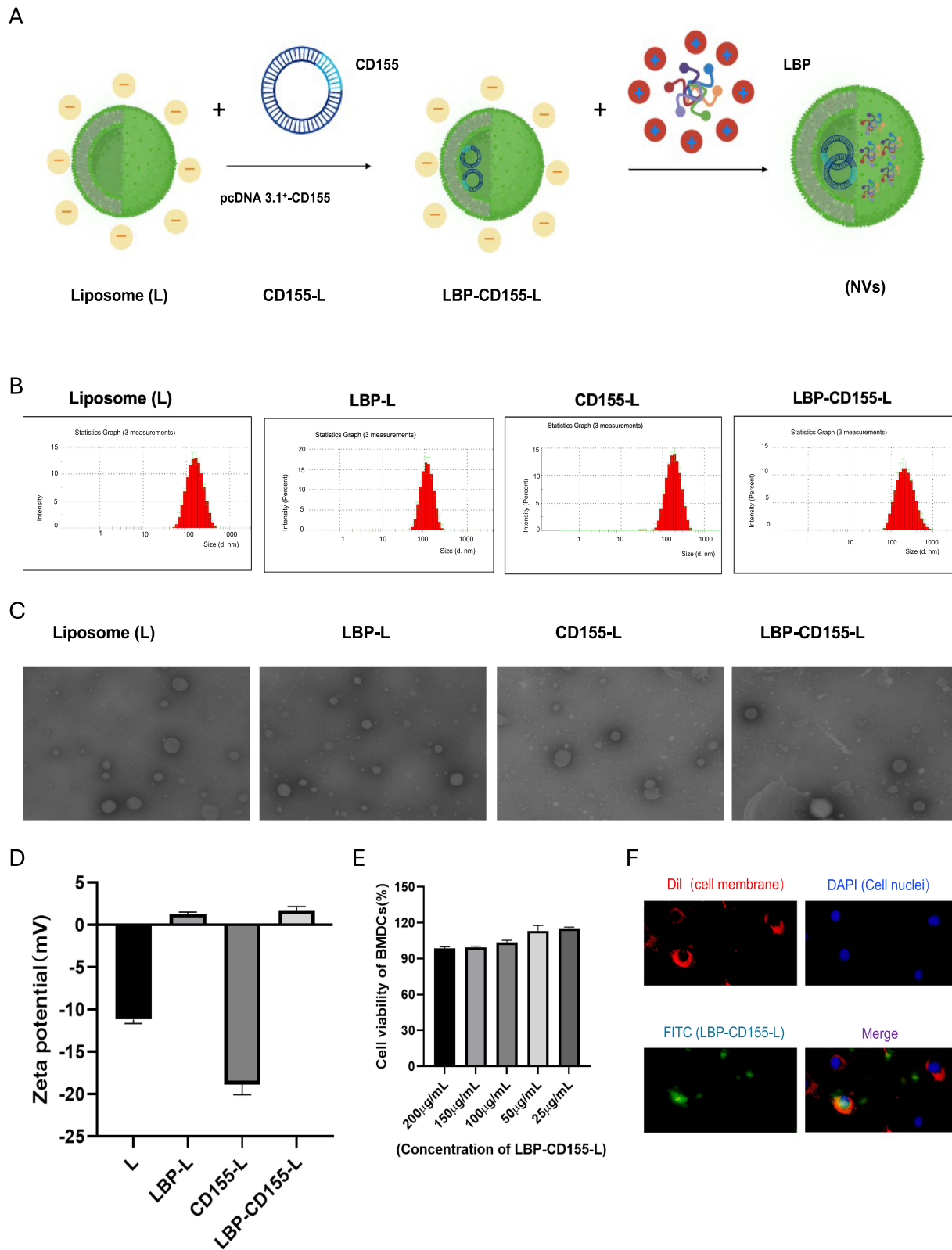


Figure 1 Synthesis and characterisation of LBP-CD155-L NVs. **(A)** Schematic illustration of the preparation of LBP-CD155-L NVs. Particle size **(B)** and Zeta potential **(D)** of different nanoparticles measured by DLS. **(C)** Transmission electron microscopy (TEM) images of LBP-CD155-L NVs. **(E)** CCK8 detection of LBP-CD155-L NVs toxicity to BMDCs (n=3). **(F)** Fluorescence microscopy images show the uptake of targeted LBP-L. After Co-incubate LBP-L with DC2.4 cells for 12h. The cell membrane was labeled with Dil (red), the LBP was stained using FITC (green) and the nuclei of the cells were stained using DAPI (blue). Original magnification 400x.

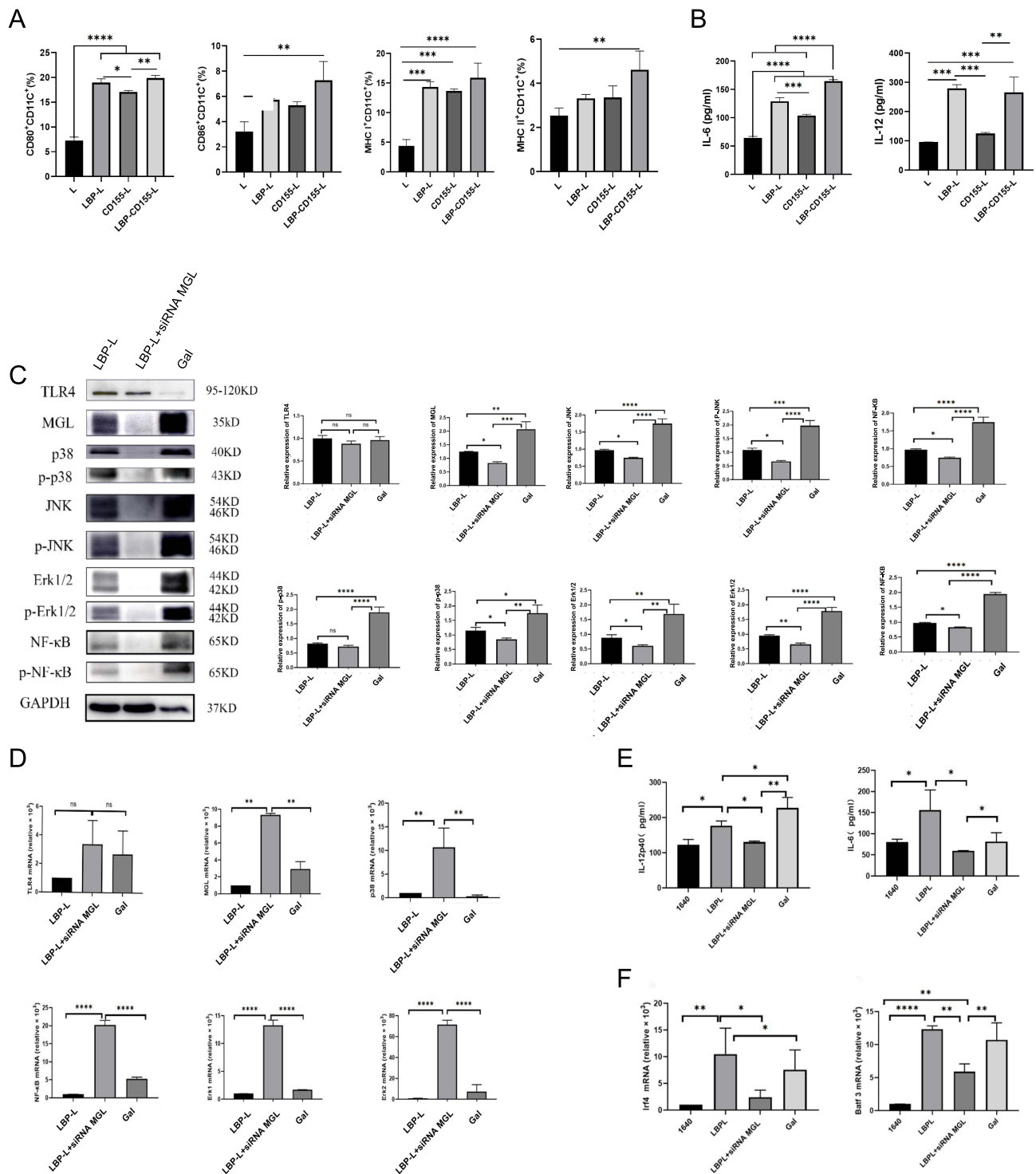


Figure 2 Nanovaccine-induced BMDCs maturation and pathways induced by nanovaccine. After different nanoparticles were coincubated with BMDCs for 24h, the expression of the costimulatory molecules CD80, CD86, MHC I and MHC II on BMDCs was detected by Flow Cytometry (A). The effect of different nanoparticles on cytokine IL-6 and IL-12p40 secretion in BMDCs was detected by ELISA Kits (B). Effects of blocking MGL on the expression of MGL and TLR4 pathways in DCs maturation. Western blotting (C) and TaqMan qPCR (D) analyze the TLR4, MGL, P38, p-P38, JNK,p-JNK, Erk1/2, p-Erk1/2, NF-κB and p-NF-κB protein levels after transfection immature DCs with 100 nM/L siRNA MGL. The cytokines IL-6 and IL-12p40 (E) were measured by ELISA Kits after transfection of immature DCs with 100 nM/L siRNA MGL. LBP-L vaccination increased cDC1 cells maturation. The TaqMan qPCR analyzes the expression levels of Irf4 and Batf3 (F) after transfection immature DCs with 100 nM/L siRNA MGL. n=3 “ns” not significant, *p < 0.05, **p < 0.01, ***p < 0.001, and ****p < 0.0001.

could be specifically recognized by saccharide receptor on DCs, thus improving the targeting to DCs and the internalization efficiency of antigens. It was found in surprise that silencing galactose-type lectins (MGL) attenuated the activation of the MAPK pathway induced by LBP, as evidenced by a significant decrease in the protein and mRNA expression levels of MGL, P38, p-P38, JNK, p-JNK, Erk1/2, p-Erk1/2, NF- κ B, and p-NF- κ B (Figure 2C and D). Furthermore, IL-12p40 and IL-6 secretion was also inhibited in MGL-silenced conditions (Figure 2E), confirming that LBP induces DC maturation through MGL binding. Additionally, it was established that LBP-modified nanoparticles could induce mRNA expression of *Batf3* and *Irf4* in DCs, representing cDC1 and cDC2, respectively, which is indicating that LBP is capable of inducing differentiation in both DC subsets and is also inhibited by silencing MGL (Figure 2F). These findings confirm that LBP induce DC maturation through the synergistic effect of MGL and TLR 4 pathways.

In Vitro Evaluation of LBP-Nanoparticles Induced DC Promoting CD8⁺T Cytotoxicity

To evaluate the activation state of cytotoxic T cells induced by BMDCs treated with LBP-modified nanoparticles. BMDCs treated with LBP-modified nanoparticles were co-cultured with mouse splenocytes at a ratio of 1:10 for 72h, and then CD8⁺T cells was detected by flow cytometry. The results indicated that the frequency of CD8⁺T cells, levels of IFN- γ and TNF- α secreted in CD8⁺T cells was increased in groups treated with LBP-modified nanoparticles (Figure 3A). In

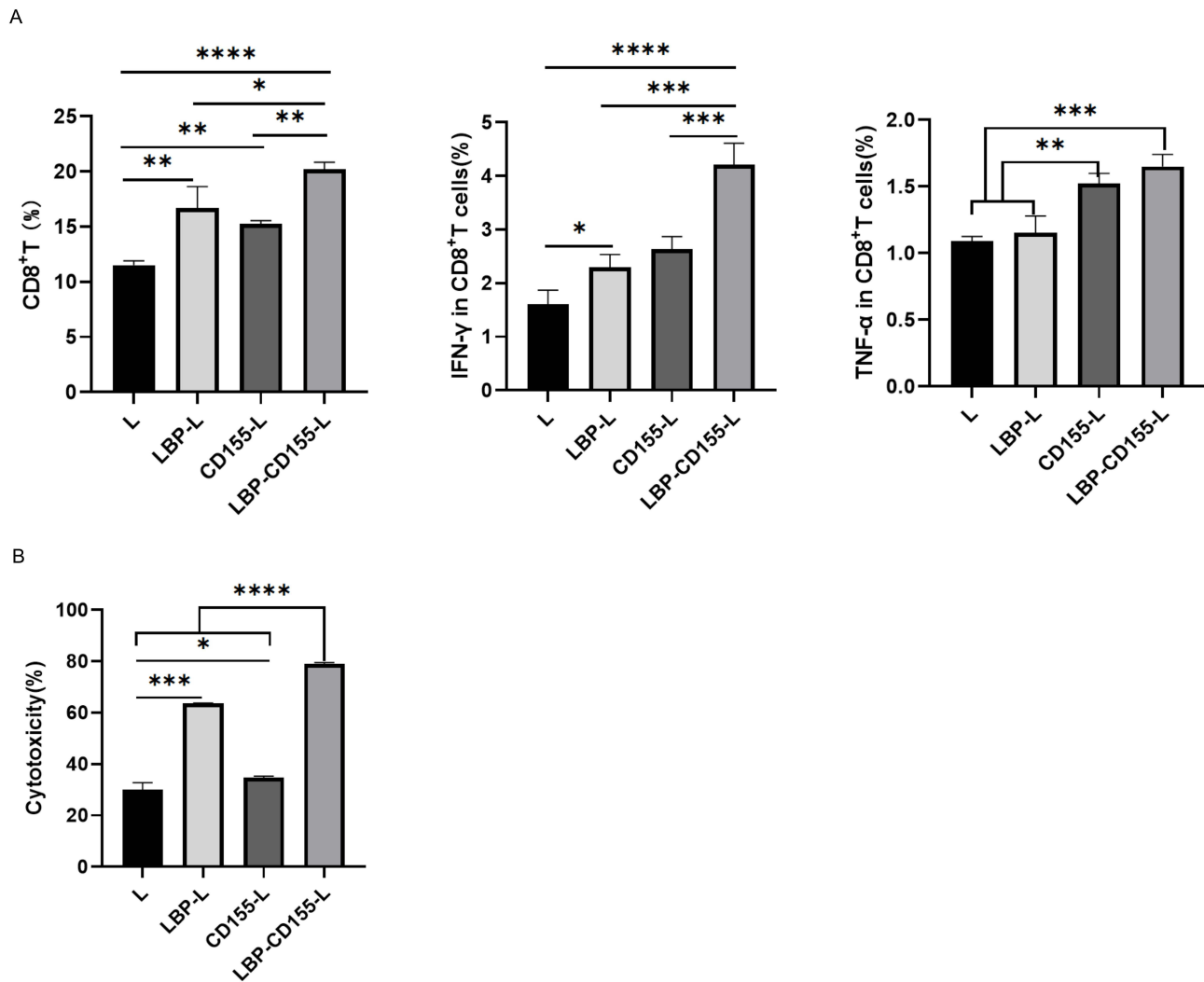


Figure 3 In vitro evaluation of nanovaccine induced DCs enhancement of CD8⁺T cell killing effects. Co-cultured nanoparticle-pulsed BMDCs with mouse spleen-derived T cells can activate CD8⁺T cell, IFN- γ CD8⁺T cells and TNF- α CD8⁺T cells (A). Nanovaccine promoting BMDCs-induced T cells activation and killing HT-29 cells. CCK8 was used to detect the killing effect on HT-29 cells after co-incubation of activated T cells with HT-29 cells at the potency-target ratio was 20:1 (B). n=3, *p < 0.05, **p < 0.01, ***p < 0.001, and ****p < 0.0001.

order to prove the superiority of the modified nanoparticles in inducing cytotoxic T cells mediated response, the cytotoxic effect of these activated T cells was further evaluated. HT-29 cells were co-cultured with the aforementioned cells at an effector-to-target ratio of 20:1 for 48h, and the cytotoxic effect of the activated lymphocytes on HT-29 cells was determined using the CCK-8 assay. Compared with liposome nanoparticles groups, the degree of apoptosis in LBP-modified nanoparticles was significantly higher (Figure 3B), which is indicating that LBP is capable of enhancing DC inducing tumor effector T cell cytotoxicity.

In Vivo Evaluation of the Prophylactic and Therapeutic Effects of LBP-CD155-L NVs

The prophylactic and therapeutic effect of LBP-modified nanoparticles loaded with CD155 (LBP-CD155-L NVs) on a transplantation tumor model utilizing human HT-29 cells in C57BL/6 mice was subsequently evaluated. The immunotherapy strategies included prevention and therapy, immunization of LBP-CD155-L NVs before and after tumor inoculation, respectively (Figure 4A). Obviously, there was no significant difference in body weight across all experimental groups (Figure 4B), indicating the safety of the antitumor strategy employed. As revealed, compared with PBS group, both the prophylactic and therapeutic administration of LBP-CD155-L NVs effectively inhibited tumor growth (Figure 4C). Further verification of the antitumor effect of LBP-CD155-L NVs was provided by tumor photography and statistical results (Figure 4D). Both the prophylactic and the therapeutic interventions by LBP-CD155-L NVs significantly increased the proportion of mature DCs in peripheral immune organs (inguinal lymph nodes and spleens) and TME (Figure 4E). In addition, consistent with in vitro results, the LBP-CD155-L NVs in both prophylactic and

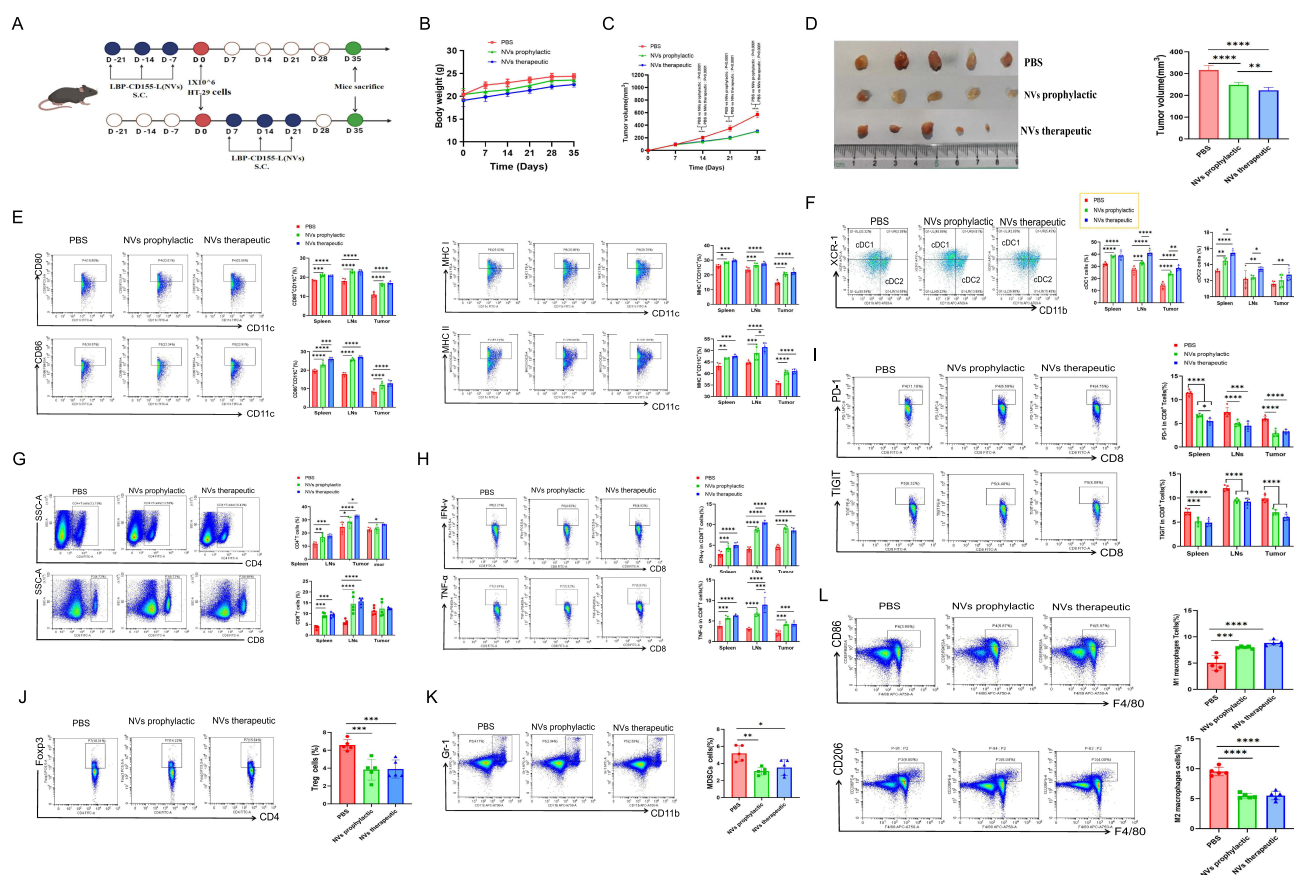


Figure 4 In vivo preventive therapeutic efficacy induced by LBP-CD155-L NVs. (A) Illustration of the schedule for evaluating the preventive and therapeutic effect in HT-29 tumor model. (B) Body weight curves of mice in each group during different treatments. Tumor volume–time curve (C). Pictures and measurement results of the tumors (D) isolated from mice on day 35 after the HT-29 cells inoculation. (E) Representative FCM plots of mature DCs in peripheral immune organs and tumour microenvironment. The frequency of DC subsets cDC1 and cDC2 (F). The frequency of CD4⁺T and CD8⁺T (G), TNF- α and IFN- γ secreted by CD8⁺T-cell infiltrates (H), the frequency of co-inhibitory molecules PD1 and TIGIT on CD8⁺T-cell (I). The frequency of immunosuppressive cells in the TEM. Tregs (CD4⁺ + FoxP3⁺) (J) and MDSCs (CD11b⁺ + Gr-1⁺) (K). M1-like macrophages (CD86⁺ + F4/80⁺) and M2-like macrophages (CD11b⁺ + F4/80⁺) (L) are shown. n=5, *p < 0.05, **p < 0.01, ***p < 0.001, and ****p < 0.0001.

therapeutic contexts promoted the maturation of DC and induced the differentiation of DC subsets. Following LBP-CD155-L NVs intervention, both cDC1 and cDC2 were significantly increased (Figure 4F). Recent studies demonstrated that cDC1 can restimulate and expand anti-cancer CD8⁺T cells by presenting tumor antigens and by secreting cytokines that regulate T cell survival and effector function in TME.^{39,40} Both prophylactic and therapeutic applications of LBP-CD155-L nanoparticles significantly enhanced the proportion of both CD8⁺ and CD4⁺ T cells in peripheral immune organs and TME (Figure 4G). Both prophylactic and therapeutic applications of LBP-CD155-L NVs increased levels of TNF- α and IFN- γ secreted by CD8⁺T cell infiltrates (Figure 4H), while decreasing the frequency of co-inhibitory molecules PD1 and TIGIT on CD8⁺T-cell (Figure 4I), indicating a restoration of CD8⁺T cells function induced by LBP-CD155-L NVs. Meanwhile, the populations of immunosuppressive cells Tregs (Figure 4J) and MDSCs (Figure 4K) in the TME significantly decreased following prophylactic and therapeutic interventions with LBP-CD155-L NVs. In addition, the macrophage phenotypes were reprogrammed by LBP-CD155-L NVs in the TME, with a significant increase in the percentage of M1-like macrophages and a remarkable decrease in M2-like macrophages (Figure 4L). This may be due to the significant immunosuppression induced by CD155, showing its potential as a therapeutic target. CD155 also exerts an anti-tumorigenic role regulating immune response to tumors thanks to its ability to interact with immune receptors on cytotoxic lymphocytes.^{41–45} Altogether, with a decrease in tumor volume, the anti-tumor immune responses triggered and immunosuppression in the TME inhibited by the LBP-CD155-L NVs offer a promising strategy for effective immunotherapy approaches of colorectal cancer.

In Vivo Evaluation of the Prophylactic and Therapeutic Effects Induced by Combination of LBP-CD155-L NVs and α PD-1

The combination dosing schedule of LBP-CD155-L NVs with anti-PD-1 (α PD-1) induced robust and safe tumour growth inhibition (Figure 5A). During the monitoring period, no apparent change in mice's body weight was observed across all groups (Figure 5B), indicating that the quality of life of mice was not influenced by different treatments. Combined application of LBP-CD155-L NVs can improve α PD-1 immune therapy efficacy, which was proved by the regression of the tumor (Figure 5C and D). The enhancing effect of combined immune therapy has been further confirmed by promoting maturation of DCs and differentiation of cDC1 subset (Figure 5E and F), and by restoring the anti-tumor immune effect of T cells (Figure 5G-I). In addition, confirming that combined immune therapy can improve immunosuppressive status of α PD-1 immune therapy through repolarization of macrophage, decreasing MDSCs and Tregs infiltration in TME (Figure 5J-L). Overall, the experimental data obtained from HT-29 colorectal tumor models verified the obvious antitumor efficacy of the combined LBP-CD155-L NVs with α PD-1 treatment offering a favorable strategy for effective colorectal tumor inhibition.

Safety Evaluation of Combination Therapy

On day 35 following the inoculation with HT-29 cells, mice were sacrificed and dissected. Tissue specimens, including the heart, liver, spleen, lung, and kidney, were harvested for further analysis. Compared to the model group, there was no significant morphological damage in the histological sections with NVs treatments (Figure 6). This outcome indicates the biosafety of LBP-modified liposome nanoparticles loaded with CD155 and underscores their potential for clinical application.

The study indeed shows the promising results of our new nanovaccine. Next steps for translating it to clinical applications will start with conducting comprehensive preclinical studies in more advanced animal models to further assess LBP's safety and efficacy profiles. Then, plan for small-scale Phase 1 human clinical trials focused on gauging safety and initial immune responses. Potential hurdles in the human immune response to LBP include the risk of triggering excessive inflammation. Whether the dose escalation will have side effects, there is also concern about potential autoimmune reactions. Understanding individual variations in immune responses will be vital. Additionally, we must study how LBP interacts with other immune components. By systematically addressing these aspects, we can go further to successful clinical translation.

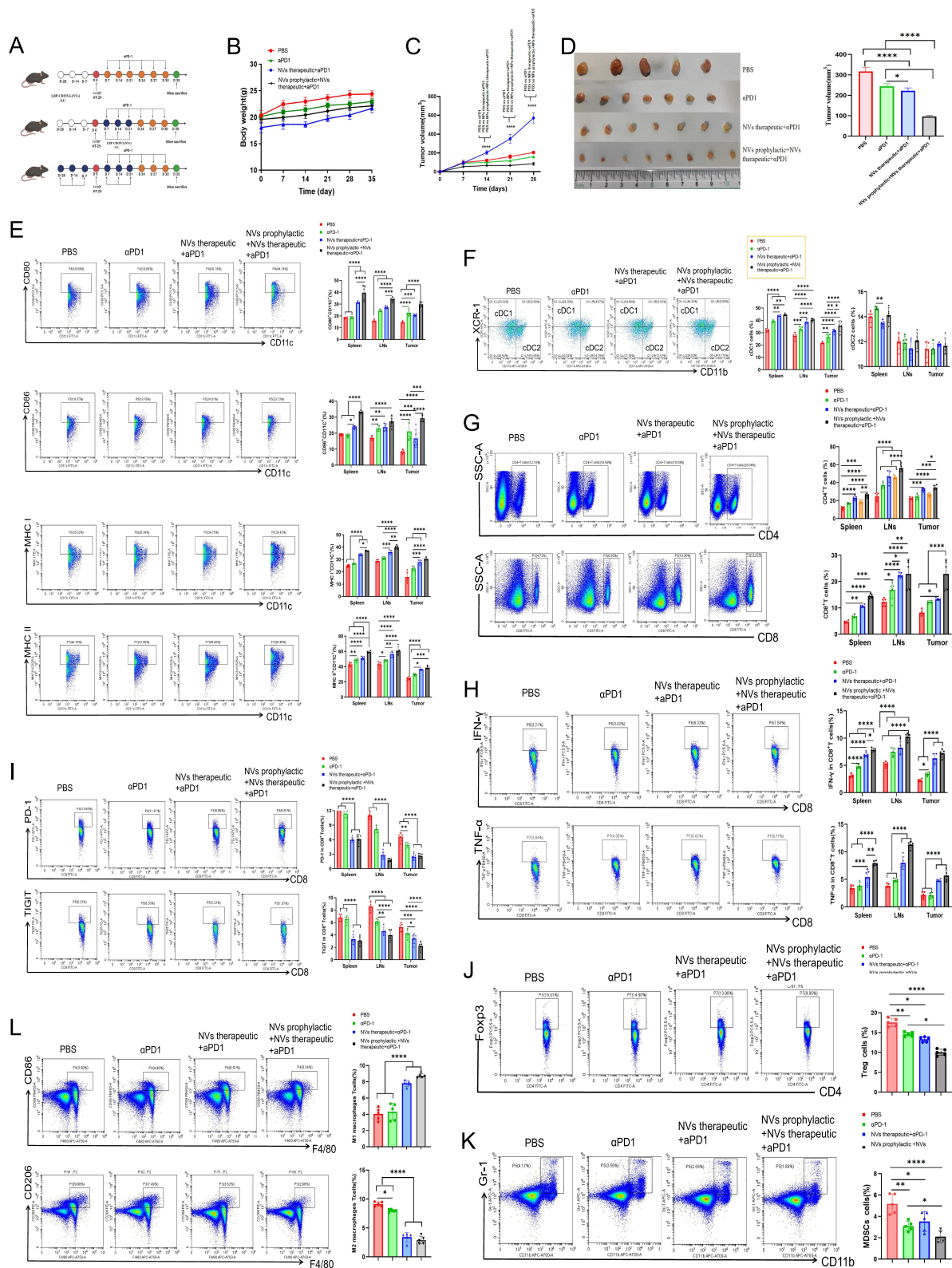


Figure 5 In vivo immune prevention and therapeutic efficacy induced by combination of LBP-CD155 NVs and aPD-I. (A) Illustration of the schedule for evaluating the LBP-CD155 NVs combination with aPD-I preventive and therapeutic effects in HT-29 transplant tumor model. (B) Body weight curves of mice in each group during different treatments (n = 8). Tumor volume-time curve (C). Pictures and measurement results of the tumors (model). (D) Pictures and measurement results of the tumors (model). (E) Representative FCM plots of mature DCs in peripheral immune organs and tumour microenvironment. The frequency of DC subsets cDC1 and cDC2 (F). The frequency of CD4⁺T and CD8⁺T (G), TNF- α and IFN- γ secreted by CD8⁺T-cell infiltrates (H), the frequency of co-inhibitory molecules PD1 and TIGIT on CD8⁺T-cell (I). The frequency of immunosuppressive cells in the TEM. Tregs (CD4⁺FoxP3⁺) (J) and MDSCs (CD11b⁺Gr-1⁺) (K). M1-like macrophages (CD86⁺F4/80⁺) and M2-like macrophages (CD11b⁺F4/80⁺) (L) are shown. n=8; *p < 0.05, **p < 0.01, ***p < 0.001, and ****p < 0.0001.

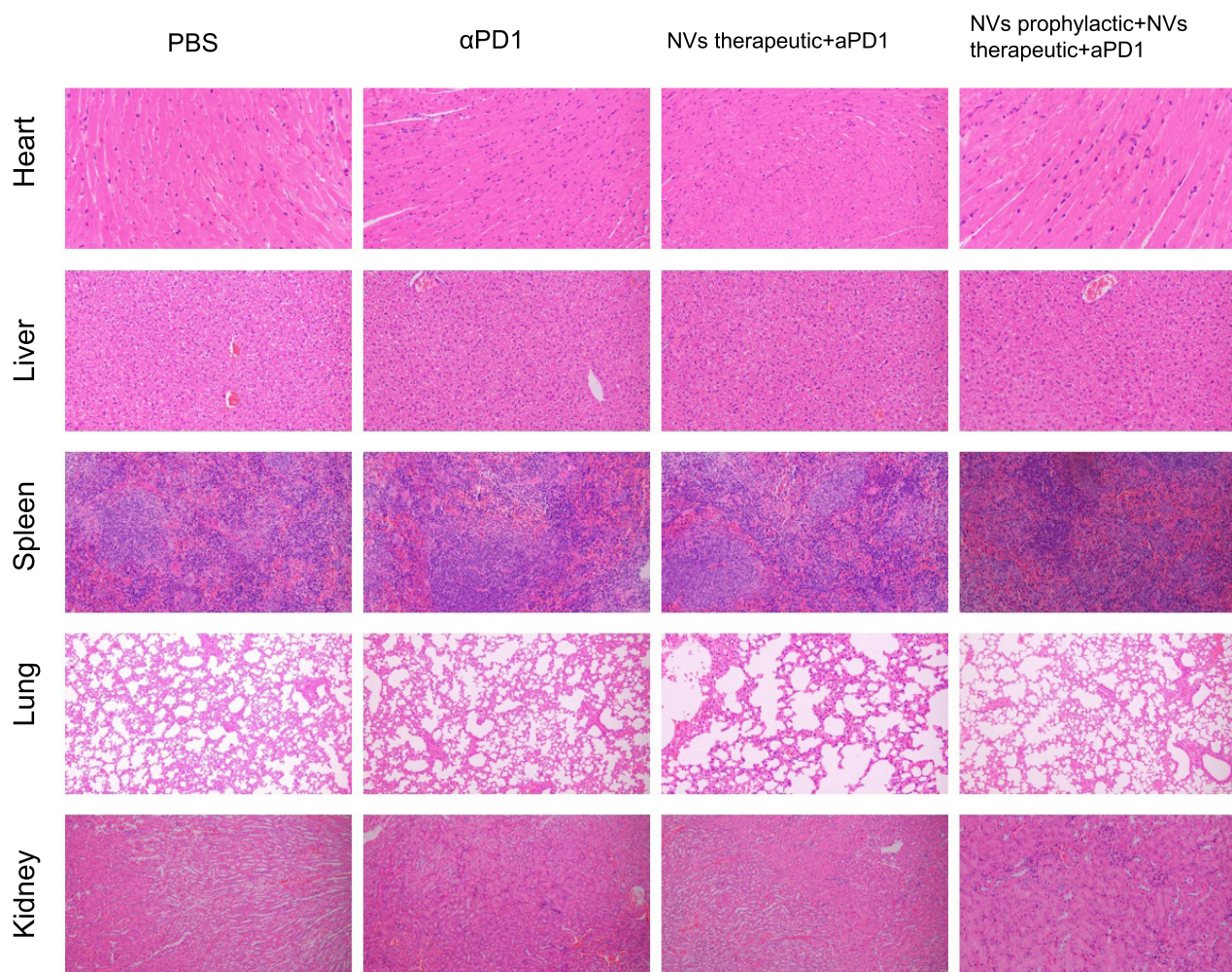


Figure 6 Safety evaluation. Hematoxylin–eosin staining (H&E staining) of the major organs including the heart, liver, spleen, lungs, and kidneys in the C57BL/6 mice model.

Conclusion

The recent clinical validation of different ICBs, such as α PD1 and α CTLA4, has revolutionized cancer therapy. However, the benefits of ICB are limited to a small subset of patients, primarily due to the lack of pre-existing target cells.⁴⁶ Hence, the identification of alternative approaches and targets that may improve responsiveness when used in combination with existing immunotherapies is a current priority. One attractive target in this context is the immune regulatory functions of the cell adhesion molecule CD155. Nanovaccines, as an active immunotherapeutic strategy, has the unique ability to expand the host antitumour-specific T-effector phenotype, thereby improving antitumor immune response. In this study, LBP was utilized as an adjuvant to construct a liposomes nanovaccine (LBP-CD155 NVs) by electrostatic interaction, capable of co-encapsulating CD155 gene and adjuvant (LBP). When it comes to the mechanism of immune modulation, LBP could target DCs surface CLRs and effectively improve the endocytosis and maturation of DCs by the synergistic pathway involving TLR4 and MGL. This facilitated the promotion of the differentiation of cDC subsets, especially cDC1s, which is critical for overcoming host tolerance to tumour cells by improving the effective T-cell priming and lymphocyte expansion. Moreover, LBP-CD155-L NVs can modulate immunosuppressor cells (MDSCs, Tregs) and promote repolarization of macrophages in the TME. Through these multiple ways of acting on the immune system components, it creates a more favorable immune microenvironment for combating tumors. Furthermore, the combination of LBP-CD155-L NVs and α PD-1 immune therapy strategy contributed to an optimal homeostasis in the TME. This approach enhances T-cell responses within the TME, inhibits immunosuppressive cells, and demonstrates significantly improved anti-tumor immune therapy efficacy. Therefore, LBP modified nanovaccine was crucial for the DC-mediated

antigen presentation and the activation of tumour-antigen-specific T cells. Looking forward, the combination of LBP-CD155-L NVs and α PD-1 immune therapy strategy paves the way for further exploration of how this combination could be optimized and translated into clinical applications. Future research could focus on investigating its long-term effects, exploring its potential in combination with other emerging immunotherapies, and determining the best strategies for its clinical implementation to benefit a wider range of cancer patients. In sum, a novel nanovaccine platform has been developed, activating the immune response and overcoming immune tolerance.

Ethical Approval and Consent to Participate

All animal studies were reviewed and approved by the Institutional Animal Care and Use Committee of Ningxia Medical University (approval number: IACUC-NYLAC-2023-161).

Consent for Publication

All authors provide consent for the publication of the manuscript detailed above.

Acknowledgments

All authors thank the respective editors and professional reviewers for their efforts on improving this manuscript during the peer review process.

Funding

This work was supported by the National Natural Science Foundation of China (No.82260819,82160548,31860695) Natural Science Foundation of Ningxia Province (No.2023AAC02042, 2023AAC02082, 2021AAC02011, 2020AAC03183) Key Research and Development Program of Ningxia Province (No.2023BEG02013).

Disclosure

The authors declare that they have no known competing financial interests or personal relationships that could have appeared to influence the work reported in this paper.

References

1. Wu Z, Li S, Zhu X. The Mechanism of Stimulating and Mobilizing the Immune System Enhancing the Anti-Tumor Immunity. *Front Immunol.* 2021;12:682435. doi:10.3389/fimmu.2021.682435
2. Yi M, Zheng X, Niu M, Zhu S, Ge H, Wu K. Combination strategies with PD-1/PD-L1 blockade: current advances and future directions. *mol Cancer.* 2022;21(1):28. doi:10.1186/s12943-021-01489-2
3. Yong SB, Chung JY, Song Y, Kim J, Ra S, Kim YH. Non-viral nano-immunotherapeutics targeting tumor microenvironmental immune cells. *Biomaterials.* 2019;219:119401. doi:10.1016/j.biomaterials.2019.119401
4. Stewart CL, Warner S, Ito K, et al. Cyoreduction for colorectal metastases: liver, lung, peritoneum, lymph nodes, bone, brain. When does it palliate, prolong survival, and potentially cure? *Curr Probl Surg.* 2018;55(9):330–379. doi:10.1067/j.cpsurg.2018.08.004
5. Weng J, Li S, Zhu Z, et al. Exploring immunotherapy in colorectal cancer. *J Hematol Oncol.* 2022;15(1):95. doi:10.1186/s13045-022-01294-4
6. CY C, Ueha S, Ishiwata Y, et al. Combined treatment with HMGN1 and anti-CD4 depleting antibody reverses T cell exhaustion and exerts robust anti-tumor effects in mice. *J Immunother Cancer.* 2019;7(1):21.
7. Lupo KB, Matosevic S. CD155 immunoregulation as a target for natural killer cell immunotherapy in glioblastoma. *J Hematol Oncol.* 2020;13(1):76. doi:10.1186/s13045-020-00913-2
8. Danisch S, Qiu Q, Seth S, et al. CD226 interaction with CD155 impacts on retention and negative selection of CD8 positive thymocytes as well as T cell differentiation to follicular helper cells in Peyer's Patches. *Immunobiology.* 2013;218(2):152–158. doi:10.1016/j.imbio.2012.02.010
9. O'Donnell JS, Madore J, Li XY, Smyth MJ. Tumor intrinsic and extrinsic immune functions of CD155. *Semin Cancer Biol.* 2020;65:189–196. doi:10.1016/j.semcancer.2019.11.013
10. Zhao H, Ma J, Lei T, Ma W, Zhang M. The bispecific anti-CD3 \times anti-CD155 antibody mediates T cell immunotherapy for human prostate cancer. *Invest New Drugs.* 2019;37(5):810–817. doi:10.1007/s10637-018-0683-9
11. Martinet L, Ferrari De Andrade L, Guillerey C, et al. DNAM-1 expression marks an alternative program of NK cell maturation. *Cell Rep.* 2015;11(1):85–97. doi:10.1016/j.celrep.2015.03.006
12. Zhang J, Zhou L, Xiang JD, Jin CS, Li MQ, He YY. Artesunate-induced ATG5-related autophagy enhances the cytotoxicity of NK92 cells on endometrial cancer cells via interactions between CD155 and CD226/TIGIT. *Int Immunopharmacol.* 2021;97:107705. doi:10.1016/j.intimp.2021.107705
13. Chan CJ, Martinet L, Gilfillan S, et al. The receptors CD96 and CD226 oppose each other in the regulation of natural killer cell functions. *Nat Immunol.* 2014;15(5):431–438. doi:10.1038/ni.2850

14. Ochiai H, Campbell SA, Archer GE, et al. Targeted therapy for glioblastoma multiforme neoplastic meningitis with intrathecal delivery of an oncolytic recombinant poliovirus. *Clin Cancer Res.* 2006;12(4):1349–1354. doi:10.1158/1078-0432.CCR-05-1595
15. Kim M, Jeong M, Hur S, et al. Engineered ionizable lipid nanoparticles for targeted delivery of RNA therapeutics into different types of cells in the liver. *Sci Adv.* 2021;7(9).
16. Mahajan S, Tang T. Polyethylenimine-DNA Nanoparticles under Endosomal Acidification and Implication to Gene Delivery. *Langmuir.* 2022;38(27):8382–8397. doi:10.1021/acs.langmuir.2c00952
17. Ewe A, Höbel S, Heine C, et al. Optimized polyethylenimine (PEI)-based nanoparticles for siRNA delivery, analyzed in vitro and in an ex vivo tumor tissue slice culture model. *Drug Deliv Transl Res.* 2017;7(2):206–216. doi:10.1007/s13346-016-0306-y
18. Sadat Tabatabaei Mirakabad F, Nejati-Koshki K, Akbarzadeh A, et al. PLGA-based nanoparticles as cancer drug delivery systems. *Asian Pac J Cancer Prev.* 2014;15(2):517–535. doi:10.7314/APJCP.2014.15.2.517
19. Xu T, Ma Y, Huang J, et al. Self-organized thermo-responsive poly (lactic-co-glycolic acid)-graft-pullulan nanoparticles for synergistic thermo-chemotherapy of tumor. *Carbohydr Polym.* 2020;237:116104. doi:10.1016/j.carbpol.2020.116104
20. Liu N, Xiao X, Zhang Z, Mao C, Wan M, Shen J. Advances in Cancer Vaccine Research. *ACS Biomater Sci Eng.* 2023;9(11):5999–6023. doi:10.1021/acsbomaterials.3c01154
21. Dotiwala F, Upadhyay AK. Next Generation Mucosal Vaccine Strategy for Respiratory Pathogens. *Vaccines.* 2023;11(10):1585. doi:10.3390/vaccines11101585
22. Zhang Z, Zhang L, Xu H. Effect of Astragalus polysaccharide in treatment of diabetes mellitus: a narrative review. *J Tradit Chin Med.* 2019;39(1):133–138.
23. Li M, Han B, Zhao H, et al. Biological active ingredients of Astragali Radix and its mechanisms in treating cardiovascular and cerebrovascular diseases. *Phytomedicine.* 2022;98:153918. doi:10.1016/j.phymed.2021.153918
24. Tang M, Cheng L, Liu Y, Wu Z, Zhang X, Luo S. Plant Polysaccharides Modulate Immune Function via the Gut Microbiome and May Have Potential in COVID-19 Therapy. *Molecules.* 2022;27(9).
25. Cordeiro AS, Alonso MJ, de la Fuente M. Nanoengineering of vaccines using natural polysaccharides. *Biotechnol Adv.* 2015;33(6):1279–1293. doi:10.1016/j.biotechadv.2015.05.010
26. Tang WM, Chan E, Kwok CY, et al. A review of the anticancer and immunomodulatory effects of Lycium barbarum fruit. *Inflammopharmacology.* 2012;20(6):307–314. doi:10.1007/s10787-011-0107-3
27. Liu C, Gu J, Ma W, et al. Lycium barbarum polysaccharide protects against ethanol-induced spermiotoxicity and testicular degeneration in Imp21 (±) mice. *Andrologia.* 2020;52(4):e13554. doi:10.1111/and.13554
28. Zhang Q, Lv X, Wu T, et al. Composition of Lycium barbarum polysaccharides and their apoptosis-inducing effect on human hepatoma SMMC-7721 cells. *Food Nutr Res.* 2015;59:28696. doi:10.3402/fnr.v59.28696
29. Su CX, Duan XG, Liang LJ, et al. Lycium barbarum polysaccharides as an adjuvant for recombinant vaccine through enhancement of humoral immunity by activating Tfh cells. *Vet Immunol Immunopathol.* 2014;158(1–2):98–104. doi:10.1016/j.vetimm.2013.05.006
30. Bo R, Liu Z, Zhang J, et al. Mechanism of Lycium barbarum polysaccharides liposomes on activating murine dendritic cells. *Carbohydr Polym.* 2019;205:540–549. doi:10.1016/j.carbpol.2018.10.057
31. Mohr N, Kappel C, Kramer S, Bros M, Grabbe S, Zentel R. Targeting cells of the immune system: mannosylated HPMA-LMA block-copolymer micelles for targeting of dendritic cells. *Nanomedicine.* 2016;11(20):2679–2697. doi:10.2217/nmm-2016-0167
32. Vázquez-Mendoza A, Carrero JC, Rodríguez-Sosa M. Parasitic infections: a role for C-type lectins receptors. *Biomed Res Int.* 2013;2013:456352. doi:10.1155/2013/456352
33. Zizzari IG, Napoletano C, Battisti F, et al. MGL Receptor and Immunity: when the Ligand Can Make the Difference. *J Immunol Res.* 2015;2015:450695. doi:10.1155/2015/450695
34. Osada N, Nagae M, Nakano M, Hirata T, Kizuka Y. Examination of differential glycoprotein preferences of N-acetylglucosaminyltransferase-IV isozymes a and b. *J Biol Chem.* 2022;298(9):102400. doi:10.1016/j.jbc.2022.102400
35. Wang B, Liu W, Li JJ, et al. A low dose cell therapy system for treating osteoarthritis: in vivo study and in vitro mechanistic investigations. *Bioact Mater.* 2022;7:478–490. doi:10.1016/j.bioactmat.2021.05.029
36. Oberländer U, Pletincx K, Döhler A, et al. Neuromelanin is an immune stimulator for dendritic cells in vitro. *BMC Neurosci.* 2011;12:116. doi:10.1186/1471-2202-12-116
37. Foti M, Granucci F, Aggujaro D, et al. Upon dendritic cell (DC) activation chemokines and chemokine receptor expression are rapidly regulated for recruitment and maintenance of DC at the inflammatory site. *Int Immunol.* 1999;11(6):979–986. doi:10.1093/intimm/11.6.979
38. Moreno Ayala MA, Campbell TF, Zhang C, et al. CXCR3 expression in regulatory T cells drives interactions with type I dendritic cells in tumors to restrict CD8(+) T cell antitumor immunity. *Immunity.* 2023;56(7):1613–1630.e1615. doi:10.1016/j.immuni.2023.06.003
39. Meiser P, Knolle MA, Hirschberger A, et al. A distinct stimulatory cDC1 subpopulation amplifies CD8(+) T cell responses in tumors for protective anti-cancer immunity. *Cancer Cell.* 2023;41(8):1498–1515.e1410. doi:10.1016/j.ccell.2023.06.008
40. Bayerl F, Meiser P, Donakonda S, et al. Tumor-derived prostaglandin E2 programs cDC1 dysfunction to impair intratumoral orchestration of anti-cancer T cell responses. *Immunity.* 2023;56(6):1341–1358.e1311. doi:10.1016/j.immuni.2023.05.011
41. Paolini R, Molfetta R. CD155 and Its Receptors as Targets for Cancer Therapy. *Int J mol Sci.* 2023;24(16):12958. doi:10.3390/ijms241612958
42. Zhou R, Chen S, Wu Q, et al. CD155 and its receptors in cancer immune escape and immunotherapy. *Cancer Lett.* 2023; 573:216381. doi:10.1016/j.canlet.2023.216381
43. Zhan M, Zhang Z, Zhao X, et al. CD155 in tumor progression and targeted therapy. *Cancer Lett.* 2022;545:215830. doi:10.1016/j.canlet.2022.215830
44. Liu L, You X, Han S, Sun Y, Zhang J, Zhang Y. CD155/TIGIT, a novel immune checkpoint in human cancers (Review). *Oncol Rep.* 2021;45(3):835–845. doi:10.3892/or.2021.7943
45. Nandi SS, Gohil T, Sawant SA, Lambe UP, Ghosh S, Jana S. CD155: a Key Receptor Playing Diversified Roles. *Curr Mol Med.* 2022;22(7):594–607. doi:10.2174/1566524021666210910112906
46. Su T, Liu X, Lin S, Cheng F, Zhu G. Ionizable polymeric nanocarriers for the codelivery of bi-adjuvant and neoantigens in combination tumor immunotherapy. *Bioact Mater.* 2023;26:169–180. doi:10.1016/j.bioactmat.2023.02.016

International Journal of Nanomedicine

Publish your work in this journal

The International Journal of Nanomedicine is an international, peer-reviewed journal focusing on the application of nanotechnology in diagnostics, therapeutics, and drug delivery systems throughout the biomedical field. This journal is indexed on PubMed Central, MedLine, CAS, SciSearch[®], Current Contents[®]/Clinical Medicine, Journal Citation Reports/Science Edition, EMBase, Scopus and the Elsevier Bibliographic databases. The manuscript management system is completely online and includes a very quick and fair peer-review system, which is all easy to use. Visit <http://www.dovepress.com/testimonials.php> to read real quotes from published authors.

Submit your manuscript here: <https://www.dovepress.com/international-journal-of-nanomedicine-journal>

Dovepress
Taylor & Francis Group